Propulsion and Energy Forum
July 28-30, 2014, Cleveland, OH
50th AIAA/ASME/SAE/ASEE Joint Propulsion Conference

Mission Analysis for a Micro RF Ion Thruster for CubeSat Orbital Maneuvers

Daniel Kolosa,[1] Sara Spangelo[2], Kristina Lemmer,[3] and Jennifer Hudson[4]
[1,3,4]*Western Michigan University, Kalamazoo, Michigan, 49008*
[2]*Jet Propulsion Laboratory, Pasadena, CA, 91109*

The performance of a micro RF ion thruster is analyzed for several CubeSat orbital maneuver strategies. Mission simulations are performed for various types of trajectory control, including thrust at perigee only; intermittent thrust for a passive, magnetically stabilized spacecraft; and constant and pulsed thrust along the velocity vector. For each case, the propulsion system efficiency and maximum orbit change are evaluated. Constraints on power, fuel mass, and mission duration are considered. The most effective combinations of thruster operational modes and trajectory control strategies are discussed.

Nomenclature

a	=	semi-major axis
alt	=	starting altitude
e	=	eccentricity
F_R	=	radial thrust acceleration
F_θ	=	tangential thrust acceleration
g_0	=	sea-level acceleration of gravity
h	=	angular momentum
I_{sp}	=	specific impulse
M	=	mean anomaly
m	=	mass
m_t	=	total mass of spacecraft (kg)
m_d	=	dry mass of spacecraft (kg)
$\dot{m}_{fp}$	=	fuel mass flow rate to power ratio
m_{req}	=	required fuel mass to escape Earth's sphere of influence
n	=	mean motion
P	=	Power
$\boldsymbol{r}$	=	orbital radius vector
r_f	=	final position radius
Re	=	radius of the Earth
t_{escape}	=	time to escape Earth's sphere of influence
T	=	thrust
$\boldsymbol{v}$	=	spacecraft velocity vector
V_{ex}	=	exhaust gas velocity (m/s)
V_0	=	initial thrust velocity
V_f	=	final thrust velocity
μ	=	Earth standard gravitational parameter
θ	=	true anomaly

[1] Graduate Student, Department of Mechanical and Aerospace Engineering, 1903 W. Michigan Ave., MS 5343.
[2] Systems Engineer, Jet Propulsion Laboratory (JPL), 4800 Oak Grove Drive, Pasadena, CA, 91109.
[3] Assistant Professor, Department of Mechanical and Aerospace Engineering, 1903 W. Michigan Ave., MS 5343.
[4] Assistant Professor, Department of Mechanical and Aerospace Engineering, 1903 W. Michigan Ave., MS 5343, AIAA Member.

I. Introduction

TO date, most CubeSats have been without propulsion systems because of size, power, and launch constraints. These spacecraft can perform only minimal maneuvering from the launch vehicle insertion orbit[1]. In recent years, several micro electric propulsion systems have been developed to enable CubeSat orbital maneuvers. This paper analyzes the orbit change capabilities of one of these new micro electric propulsion systems, the Busek 1cm micro RF ion thruster (BRFIT-1), for various orbit control strategies. We also compare the orbit maneuver capabilities of several other micro propulsion systems and discuss thruster effectiveness for various mission goals.

This analysis will focus on orbit-raising maneuvers initiated at Low Earth Orbit (LEO). For these maneuvers, the thrust vector is constrained to lie in the orbital plane, aligned with the orbital velocity vector. Two basic cases of trajectory control are considered: constant thrust along the velocity vector and thrust along the velocity vector near perigee only. The constant thrust case requires 3-axis attitude control to maintain body alignment with the velocity vector. This case typically yields the fastest orbit changes, but requires a 3-axis attitude control system to maintain thruster pointing.

Thrust at perigee represents the most fuel-efficient scheme for orbit-raising maneuvers. However, with the low thrust levels of the Busek micro ion thruster (30-150 μN)[2], orbit changes will be very slow. This control could be accomplished using passive magnetic stabilization, a relatively low-complexity CubeSat attitude control strategy in which onboard magnets maintain spacecraft alignment with the Earth's gravitational fields. Orbital maneuvers of this type might be the easiest to implement on CubeSats.

After analyzing the two basic control cases, we also consider an optimized approach. Here, thrust and coast arcs are allowed to vary and the trajectory is optimized for minimal time or fuel to orbit.

An analysis of similar control strategies has been performed for the CubeSat Ambipolar Thruster (CAT)[3], and found that Earth escape is feasible for a CubeSat. That study demonstrated that maximizing altitude increase is not equivalent to maximizing thruster ΔV. Follow-on work compared conventional constant-thrusting spiral-out approaches to optimal thrusting near perigee[4]. This work considered system-level constraints such as volume, mass, power management, and radiation exposure, and determined that the optimal approach depends greatly on the system objectives and constraints. As such, mission analysis and trajectory simulations are required to quantify and compare the effectiveness of different micro propulsion systems.

The BRFIT-1 is the baseline thruster considered in this study. Its performance is evaluated for a range of thrust, power, and specific impulse values and for multiple control strategies. Following this analysis, seven other thrusters are considered using standard ΔV metrics and trajectory simulations. Fuel mass and volume constraints for a typical 3U CubeSat configuration are also considered.

A systems-level perspective that considers realistic vehicle as well as operational constraints is critical to ensure relevance of proposed solutions to realistic mission scenarios. Small spacecraft, and specifically CubeSats, are extremely mass and volume constrained. For example, the most common CubeSat size, a 3 U, is constrained to the form-factor of approximately 30 cm x 10 cm x 10 cm, and usually constrained to a mass of less than 5 kg, particularly to satisfy the standard Poly-PicoSatellite Orbital Deployer (P-POD) launcher system. These constraints influence the selection of the thruster, fuel tank, fuel, and any supporting batteries and power system components.

CubeSats are constrained in their ability to collect, store, and distribute power. Typical CubeSats that have flown in LEO with body-mounted solar panels generate less than 10 W, while spacecraft with state-of-the-art deployable panels and the ability to continually point them at the Sun may be able to generate up to 30 W. Furthermore, on-board CubeSat battery systems typically store only 50-100 kJoules and existing CubeSat electric power systems (EPSs) typically support systems that require 10-20 W. Thus, although collecting power and storing the energy for high-powered short-duration thrusts may be feasible, supplemental battery and power management systems may be required to support these types of maneuvers (which require additional volume, mass, cost, and complexity). The typical Lithium-Ion batteries that fly on CubeSat systems experience significant battery degradation[4] throughout their operation, limiting their ability to support multiple hundred cycles on longer-duration missions.

Finally, radiation is often a concern for CubeSat missions because the low-cost commercial off-the-shelf (COTS) components are typically not radiation-tolerant, thus susceptible to failures and can't reliably support long-duration missions. Mission trajectories are preferred that avoid the radiation belts as much as possible, either by operating at polar (instead of equatorial) inclinations, or by boosting their orbits to high altitudes quickly to avoid radiation exposure.

The objectives of this paper are (1) to estimate the orbital maneuver capabilities of the Busek micro ion thruster and (2) to examine the most effective operational modes of electric propulsion systems on CubeSats. We find that there is not one singular best control strategy for CubeSat maneuvers; different mission objectives are best satisfied

by different thruster properties and controls. After evaluating the BRFIT-1 and the seven trade thrusters on several metrics, we propose a map of these micro propulsion systems to the types of missions for which they are best suited.

II. Propulsion Systems

The baseline thruster for this study, the Busek BRFIT-1, has been developed and tested in a laboratory environment. It is a 1-cm-diameter gridded ion thruster that uses an inductively coupled plasma source to provide the ionization source. Thrust and specific impulse have been estimated as a function of input power and xenon gas flow rate; Table 1 shows BRFIT-1 performance data extrapolated from these tests[2]. A thruster life of over 20,000 hours (2.3 years) total operating time is expected based on a life limitation due to erosion of the grids.

Table 1. BRFIT-1 estimated properties used for trajectory simulation[2].

Power (W)	Flow Rate (sccm)	Thrust (mN)	Isp (s)
10	0.02	0.040	2000
	0.08	0.070	900
18	0.02	0.085	4400
	0.04	0.125	3200
	0.08	0.150	2000

Seven other thrusters are also considered: the VACCO/JPL Butane Micro-Thruster (cold gas thruster), the MPS-120 CubeSat High-Impulse Adaptable Modular Propulsion System (CHAMPS) (hydrazine monopropellant thruster), the Busek Green Monopropellant Thruster in both 3U and 6U versions, the Busek Micro-Resistojet (MRJ), the Busek Electrospray Thruster, and CubeSat Ambipolar Thruster (CAT) (permanent magnet helicon generated plasma thruster). The thrust, specific impulse, and average and maximum power levels of these thrusters, obtained from literature and manufacturer web sites, are given in Table 2.

Table 2. Trade thruster estimated properties.

Thruster	Thrust (mN)	Isp (s)	Avg Power (W)	Max Power (W)
VACCO/JPL Butane Micro-Thruster[5]	10-25	70	0.1	4
MPS-120 CubeSat High-Impulse Adaptable Modular Propulsion System (CHAMPS)[6 7]	260-2790	200	1	4
Busek Green Monopropellant Thruster (3U and 6U)[8]	500	230	20	20
Busek Micro-Resistojet (MRJ)[9]	2-10	150	3	3
Busek Electrospray Thruster[10]	0.7	800	3	3
CubeSat Ambipolar Thruster (CAT)[11]	0.3-32	1010	3	300

III. Control Strategies

We consider two types of trajectory control: constant thrust and perigee thrust. CubeSat attitude control requirements are different for each type, so the trajectory control strategy and spacecraft complexity are closely linked. The systems engineering issues associated with each control strategy are discussed below.

A. Constant Thrust

Constant thrust along the velocity vector requires precise 3-axis CubeSat attitude control. Reaction wheels or other developmental attitude control technology may make this control strategy feasible. Alternatively, thrust vectoring is under consideration as a means to achieve thruster pointing independent of spacecraft attitude. However, to the authors' knowledge, thrust vectoring technology does not yet exist for CubeSats with micro ion thrusters.

In the constant-thrust scheme, the need to continually provide power can be challenging for a CubeSat because in most Earth orbits, about one third of the time is in eclipse (e.g. approximately 35% with an altitude of 700 km) [4]. Therefore, the available power must be scaled by the fraction of time spent in the Sun. There are some exceptions, such as Sun-synchronous orbits, which may be able to use nearly all available power (10-30 W for a 3U CubeSat) to power the thruster while in the Sun. Furthermore, once significant orbit-raising has been achieved, the fraction and total duration of time spent in eclipse is reduced significantly (e.g. approximately 12% with an altitude of 10,000 km). Furthermore, the need to continually provide power for constant thrusting can be challenging for power system, and can make performing other functions, such as payload operations or uploading/downloading, challenging.

B. Thrust Near Perigee

The most fuel-efficient control strategy is to thrust only at perigee. In this scheme, the thruster is only active for a small fraction of each orbit, for example 5-10 minutes near closest Earth approach. Low-thrust orbital maneuvers often require long timespans, on the order of many months or years. Thruster wear and lifetime considerations are most significant for this control scheme.

Some CubeSats employ a passive magnetic stabilization strategy for attitude control, in which magnets onboard the spacecraft maintain body alignment with the Earth's magnetic field. Assuming no thrust vectoring capability, the thrust vector is aligned with the CubeSat body. As the spacecraft orbits the Earth, the thrust axis aligns with the velocity vector twice per revolution. The thruster can be oriented on the spacecraft such that it points in the velocity direction at perigee, so boosting only occurs once per orbit. This control scheme is likely the simplest to implement on CubeSats, where cost and complexity are key constraints. However, magnetic interference between the attitude control system and the ion thruster may occur. Furthermore, due to the inability to control attitude, the thrusting will not be perfectly aligned with the velocity vector, which may cause imperfect orbit-raising. This type of control will also require careful power collection and management in order to support the high-powered maneuvers at perigee.

C. Pulsed Thrust

On larger spacecraft, fuel-optimal, low-thrust spiral orbit controls typically employ intermittent thrust and coast arcs with changes in thrust direction (see, for example, the trajectory of the SMART-1 spacecraft[12]). We develop an optimized trajectory of this type for one CubeSat case. Power and thrust duration are varied within operational limits to minimize mission time. This strategy can achieve faster orbit changes than the perigee thrust case with lower fuel requirements than the constant thrust case.

IV. Simulation Methods

The initial trajectory simulations are based on the restricted two-body model of orbital motion, where a spacecraft of negligible mass orbits a large central body. The classical Newtonian equations of motion in Cartesian coordinates,

$$\dot{\boldsymbol{r}} = \boldsymbol{v}, \tag{1}$$

$$\dot{\boldsymbol{v}} = -\frac{\mu}{r^3}\boldsymbol{r} + \frac{\boldsymbol{T}}{m}, \tag{2}$$

describe this motion. However, these equations can be slow to integrate numerically due to the large variations in spacecraft position.

The Lagrange planetary equations provide an equivalent description of the two-body problem in terms of the osculating orbital elements and a perturbing thrust acceleration. The Gauss form of the Lagrange planetary equations[13] is:

$$\dot{a} = \frac{2na^2}{\mu}\left[F_R a \frac{e}{\sqrt{1-e^2}} sin\theta + F_\theta \frac{a^2}{R}\sqrt{1-e^2}\right], \tag{3}$$

$$\dot{e} = \frac{na^2}{\mu}\sqrt{1-e^2}[F_R sin\theta + F_\theta(cos\theta + cosE)], \tag{4}$$

$$\dot{\tilde{\omega}} = \frac{na^2}{\mu e}\sqrt{1-e^2}\left[-F_R cos\theta + F_\theta\left(1-\frac{r}{p}\right)sin\theta\right], \tag{5}$$

$$\dot{M} = n - \frac{2nar}{\mu}F_R + \left(1-\sqrt{1-e^2}\right)\dot{\tilde{\omega}}. \tag{6}$$

We consider only planar problems in this paper, so we exclude the Gauss equations for orbital inclination and longitude of the ascending node.

An additional differential equation is needed to calculate spacecraft mass:

$$\dot{m} = -\frac{T}{I_{sp} g_0}. \tag{7}$$

Equations (3)-(7) were integrated numerically using the MATLAB® *ode45* function, a differential equation solver that uses a Runge-Kutta method. The spacecraft was initialized in a 500 km near-circular ($e = 10^{-5}$) orbit with an initial mass of 5 kg. In the constant thrust case, the thrust was applied continuously in the direction of the velocity vector,

$$\hat{v} = \frac{1}{v}\left(\frac{h}{r}\hat{\theta} + \frac{\mu}{h} e sin\theta \hat{r}\right). \tag{8}$$

In the perigee thrust case, the thrust was applied in the direction of the velocity vector only when the true anomaly was less than 40°.

The BRFIT-1 simulations (Section V) were terminated when the spacecraft reached a radius of 925,000 km, the radius of the Earth's sphere of influence. The other thruster simulations (Section VII B) were terminated when all of the fuel was expended.

V. BRFIT-1 Simulation Results

The baseline Busek 1 cm ion thruster, the BRFIT-1, was simulated using the constant and perigee thrust strategies at the power levels and flow rates given in Table 1. Figure 1-5 show the resulting trajectories; Figure 1 and Figure 3 show orbital radius versus time, Figure 2 and Figure 4 show total spacecraft mass versus orbital radius, and Figure 5 shows the resulting spiral trajectories. The calculated time and fuel to reach geosynchronous Earth orbit (GEO), the Earth-Moon L_1 Lagrange point, the mean Moon orbit radius, and the radius of the Earth's sphere of influence are given in Table 7 in the Appendix.

The constant thrust case at 18 W power and 0.08 sccm flow rate is the fastest escape trajectory; it escapes the Earth's sphere of influence in approximately 6.2 years with 1.5 kg of fuel. However, this trajectory significantly exceeds the BRFIT-1 operating lifetime of 2.3 years. The cases of lower power, lower flow rate, and perigee thrust all require longer mission times.

Closer targets, such as GEO, can be reached in shorter times. The 18 W power, 0.08 sccm flow rate, constant thrust trajectory reaches GEO in 4.1 years, which still exceeds the thruster lifetime. The perigee thrust case for the same power and flow rate requires 28 years to reach GEO; however, the thruster does not operate continuously in this case. In this initial simulation, when thrust was only applied when the spacecraft was within 40° of perigee, the total thrusting time was approximately 2.4 years. This is close to the operating lifetime of the thruster. However, 28 years is an infeasible mission length for a CubeSat, due to radiation exposure and battery degradation.

These initial simulations indicate that an intermediate control strategy between constant thrust and perigee thrust could achieve feasible LEO-GEO transfers with the BRFIT-1. By making optimal use of power and thrust capability during portions of the trajectory where thrusting is most effective, the CubeSat could reach GEO with shorter mission duration than the perigee thrust case, but within the operating lifetime of the thruster. An optimized control strategy of this type is described in Section VI.

Although the trajectories in Figure 1-5 represent infeasible missions, the various cases' relative time and fuel requirements illustrate the trade space of power, flow rate, and control strategy. For continuous thrust, the highest power and highest flow rate case achieves the fastest orbit change. The low power/high flow rate and high power/low flow rate cases have similar radius versus time profiles, but the high power/low flow rate case uses significantly less fuel. For perigee thrust, the flight times are much longer, but fuel requirements are lower.

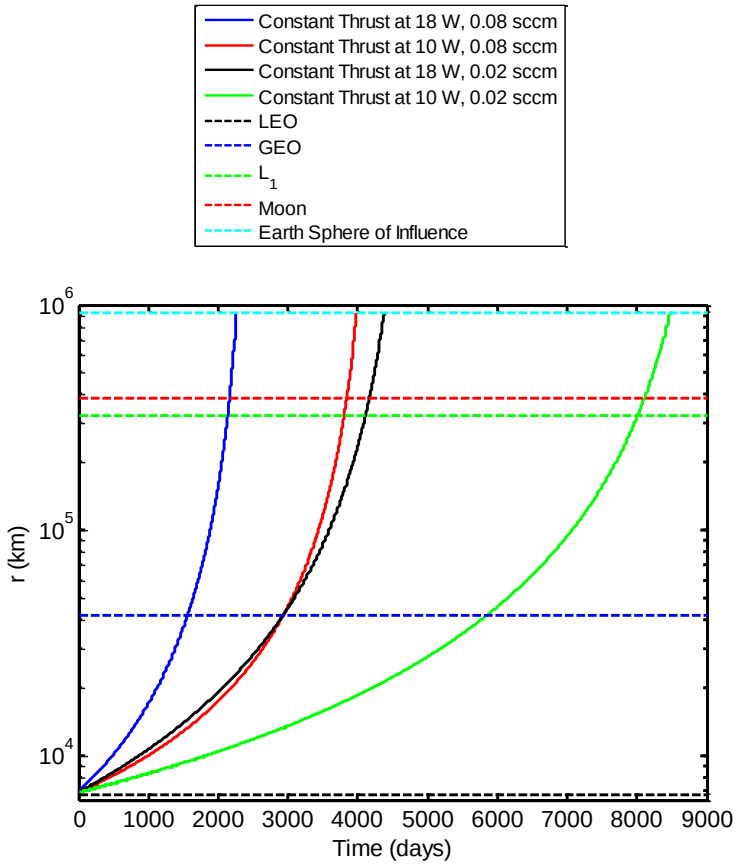

Figure 1. Radial distance versus time for the BRFIT-1 at various power levels and flow rates for constant thrust.

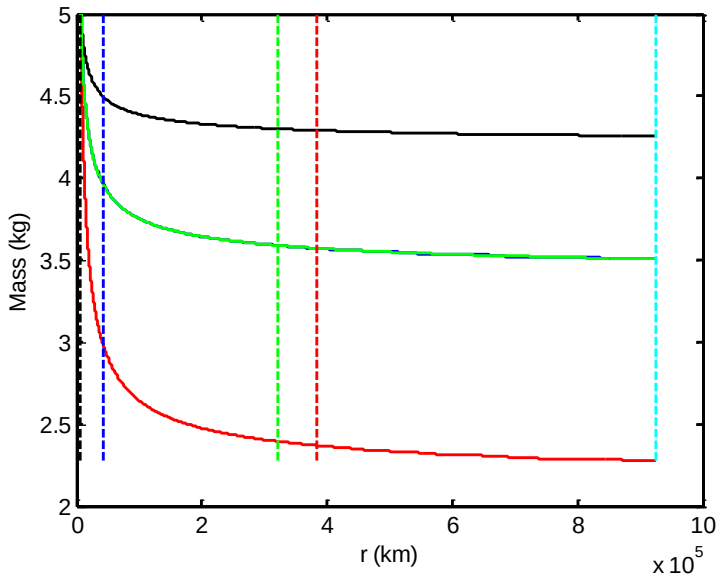

Figure 2. Mass versus radial distance for the BRFIT-1 at various power levels and flow rates for constant thrust. Note that the 18W, 0.08 sccm trajectory (blue) and the 10W, 0.02 sccm trajectory (green) overlap.

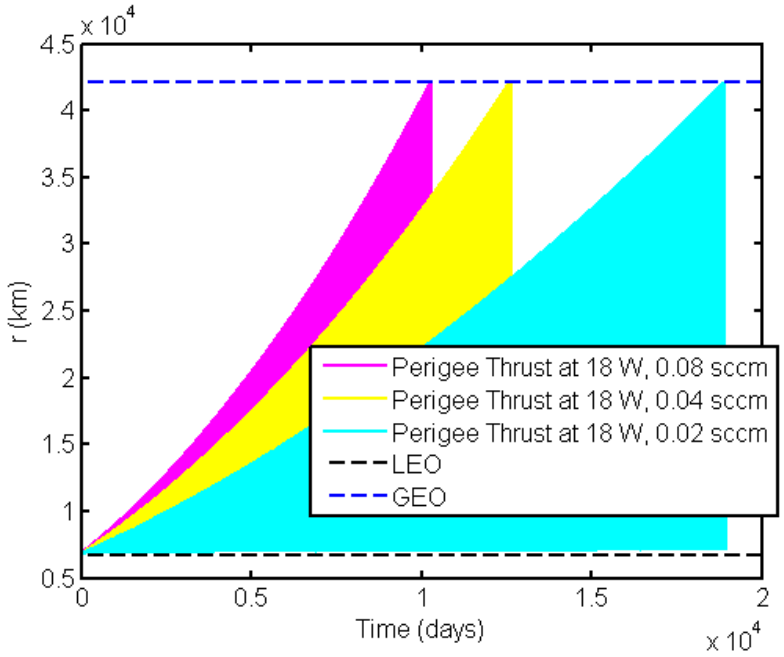

Figure 3. Radial distance versus time for the BRFIT-1 at three flow rates for perigee thrust

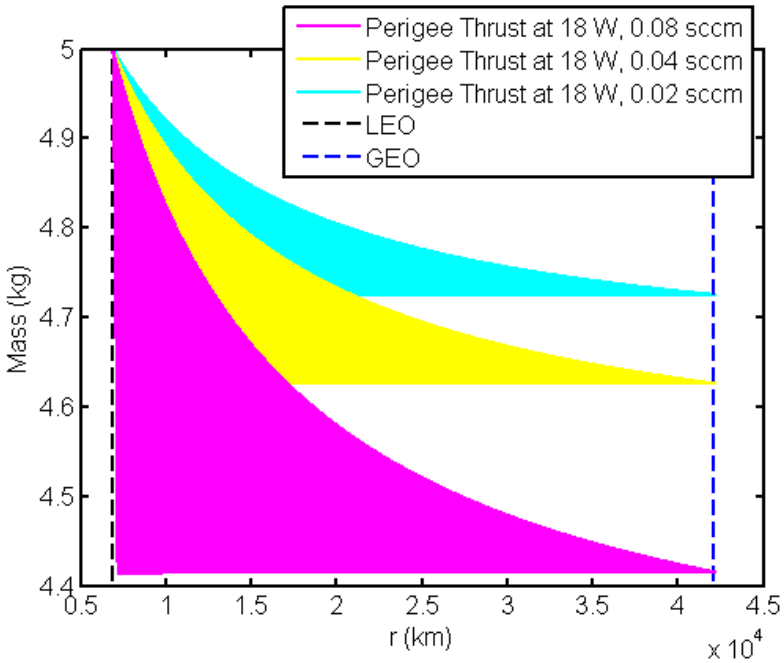

Figure 4. Mass versus radial distance for the BRFIT-1 at three flow rates for perigee thrust.

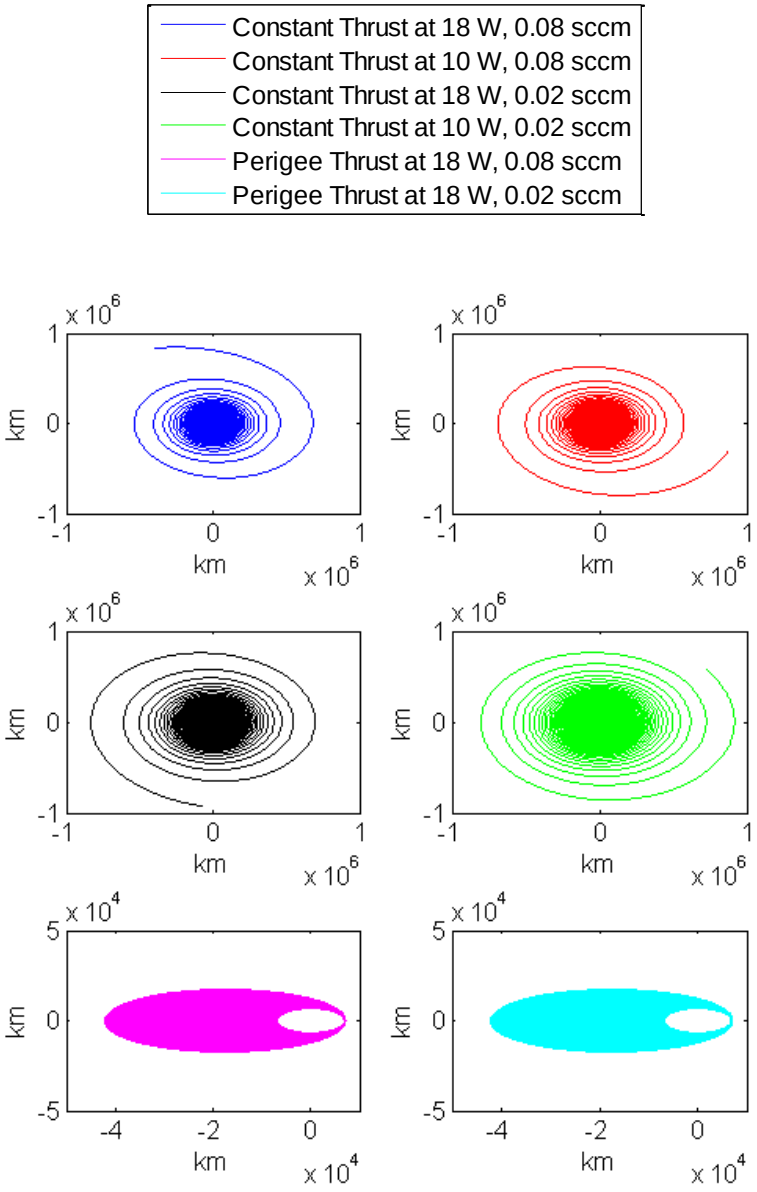

Figure 5. Planar trajectories for the BRFIT-1 at various power levels, flow rates, and control strategies.

VI. Optimized Trajectory

The thrust at perigee approach investigated in the previous section can provide significant fuel savings relative to a constant-thrust approach; however assigning a constant thrust level and duration for every orbit will likely yield sub-optimal solutions. This is because it does not allow the trajectory to benefit from the additional energy that becomes available as the spacecraft spirals from the Earth and has shorter relative eclipse times. In addition, there may be more efficient times in the mission for higher-powered or longer duration thrusts due to changes in system mass, orbit velocity, and battery capacity (as it degrades throughout the mission with greater charge/discharge cycles). Therefore, an optimal control that allows for dynamic thrust magnitude and duration may yield improvements in fuel and/or time efficiency in orbit-boosting maneuvers[4].

An analytic formulation to optimize the approach for dynamic perigee thrusting for orbit boosting has been proposed[4], where the objective function is to minimize the time required to achieve a change in orbit (i.e. LEO to GEO, LEO to Earth escape) and the model includes realistic system-level models and constraints for the spacecraft vehicle, energy, and battery. The decision variables are the level and duration of the thrust, centered at perigee, where one thrust maneuver is assumed to occur every orbital period. The formulation includes simple, analytic, and integrated models for orbit, propulsion, energy, and battery degradation. Energy constraints are enforced to ensure there is a positive energy balance every orbit, and the battery capacity, which varies dynamically as the battery degrades with additional battery cycling, is sufficient to support the thrust maneuvers and eclipses, which also vary dynamically as the orbit changes. Realistic CubeSat vehicle volume and mass constraints are also enforced (assuming a 3U CubeSat), which must account for additional batteries to supplement a nominal on-board battery, the thruster, propellant tank, and propellant.

The continuous-time problem is discretized into orbit-long intervals, where the dynamics and constraints are enforced over every orbit, and the formulation is implemented in MATLAB® and solved with *fmincon*, a solver for constrained multivariable functions. We optimize the time to transfer a spacecraft from an initial 500 km circular (non Sun-synchronous) orbit to GEO using the BRFIT-1 thruster (at 0.04 sccm), assuming an initial total mass of 5kg. We assume the spacecraft can collect up to 30 W continuously when in the Sun and that nominal operations consume an average of 3W continuously. With the optimal thrusting approach, the apogee reaches GEO in about 7.3 years and requires only 0.4 kg of fuel. Properties of the optimal solution are shown in Figure 6, where the increase in perigee velocity and apogee altitude are significant at the start of the mission, and then grow at reduced levels later in the mission. The mass decreases gradually, and the cumulative change in Δ V is only 2.75 km/sec by the time the spacecraft reaches GEO (note this is less than the nominal 3.08 km/sec required to reach GEO with the constant-thrust approach).

Operating a CubeSat for an extended period of time, over 7 years, may not be realistic given the lifetime constraints and potential failures with low-cost CubeSat-class components. This optimal result requires significantly longer to reach GEO than the constant thrust approach, but with less fuel and a total thrusting time within the thruster's lifetime constraint (compared to the infeasible total thrust time of 4 years for the fastest constant-thrust case). Compared to the case of thrusting at perigee at a fixed thrust level, which takes 30 years and 0.36 kg of fuel to reach GEO at 0.04 sccm, the optimal result is significantly faster and uses a comparable amount of fuel.

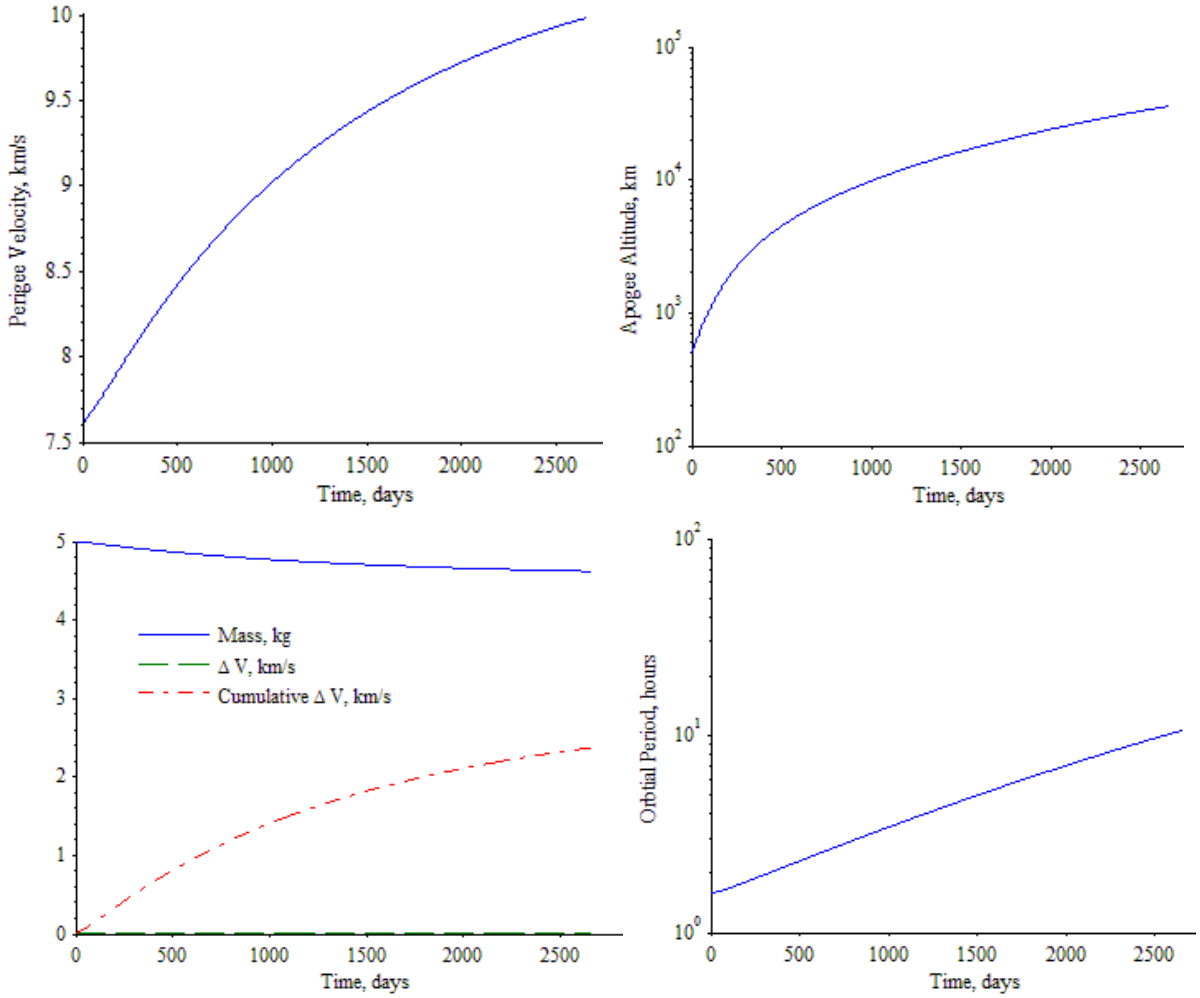

Figure 6: Properties of Optimal Thrust Solutions for BRFIT-1 Thruster for Transfer from LEO to GEO

VII. Thruster Trade Studies

A. Mass, and Volume, and ΔV Analysis

Aside from the Busek BRFIT-1, seven other thrusters were considered for CubeSat orbital maneuvers. All of these thrusters vary in propellant type, thrust, power, and I_{sp}. First, the ΔV and fuel over a range of thrust and power levels were compared. From a systems point of view, we compared the mass of each thruster relative to thrust and power.

Figure 7 shows the mass of the BRFIT-1 is average compared to the other thrusters, but the power range is higher than the other thrusters that have a similar weight. Figure 8 indicates that the BRFIT-1 has a relatively lower thrust range compared to the other seven thrusters. Figure 9 and Figure 10 compare the thrust and power ranges of all of the thrusters over I_{sp}. The BRFIT-1 has the highest I_{sp} of the selected thrusters.

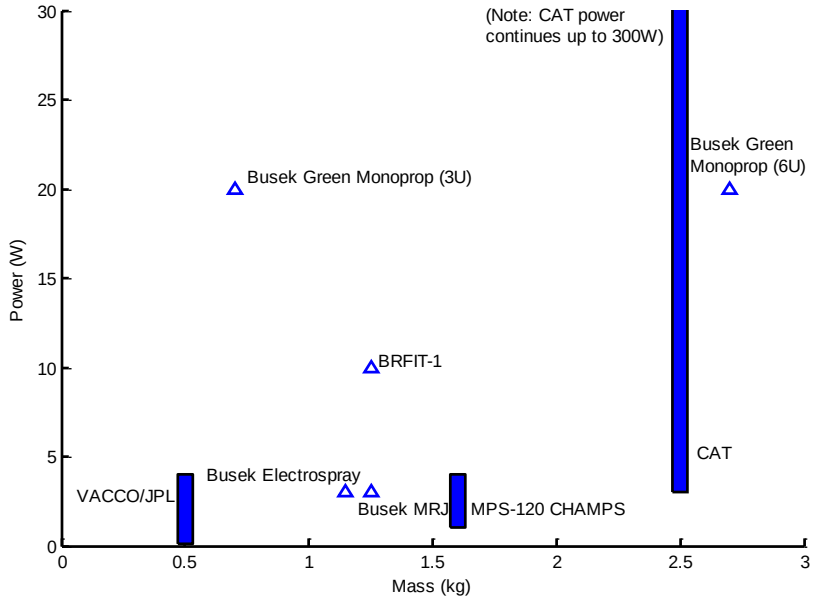

Figure 7. Mass versus power for all thrusters.

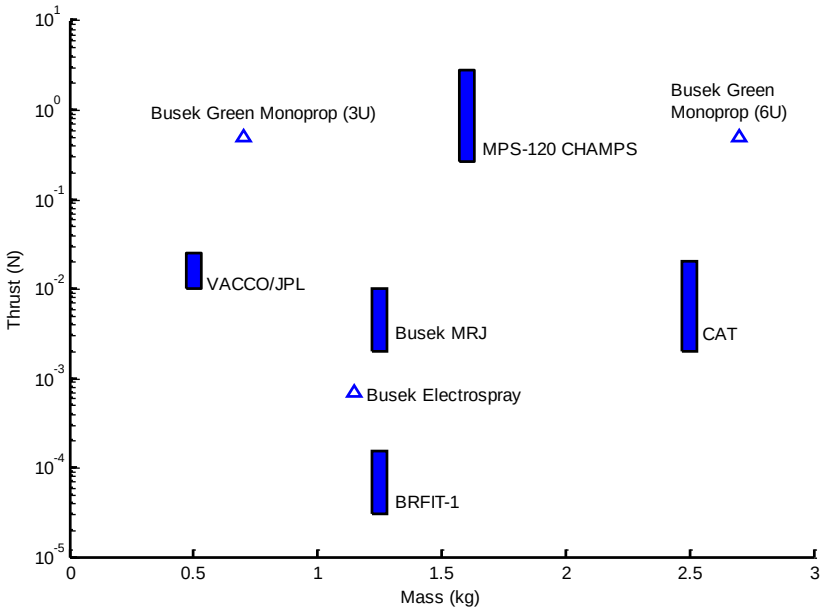

Figure 8. Thrust vs. mass for all thrusters.

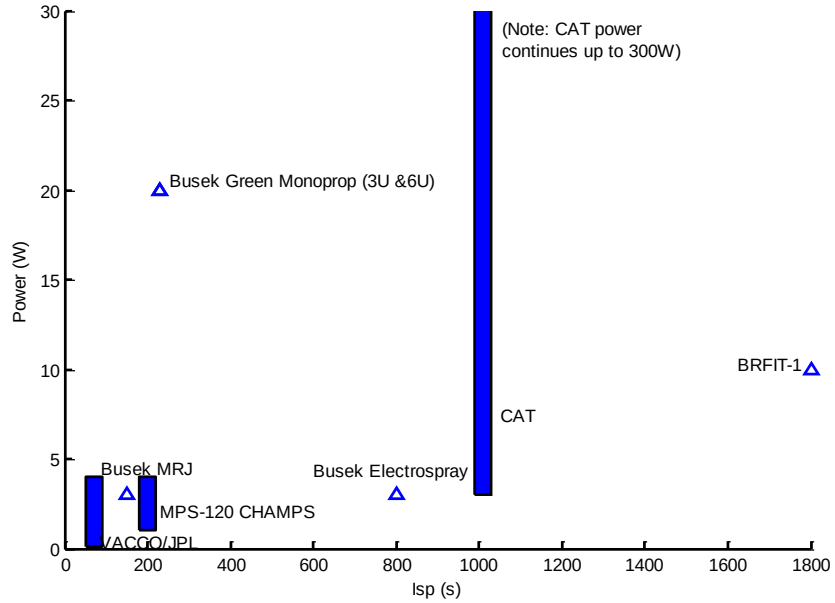

Figure 9. Power vs. Isp for all thrusters.

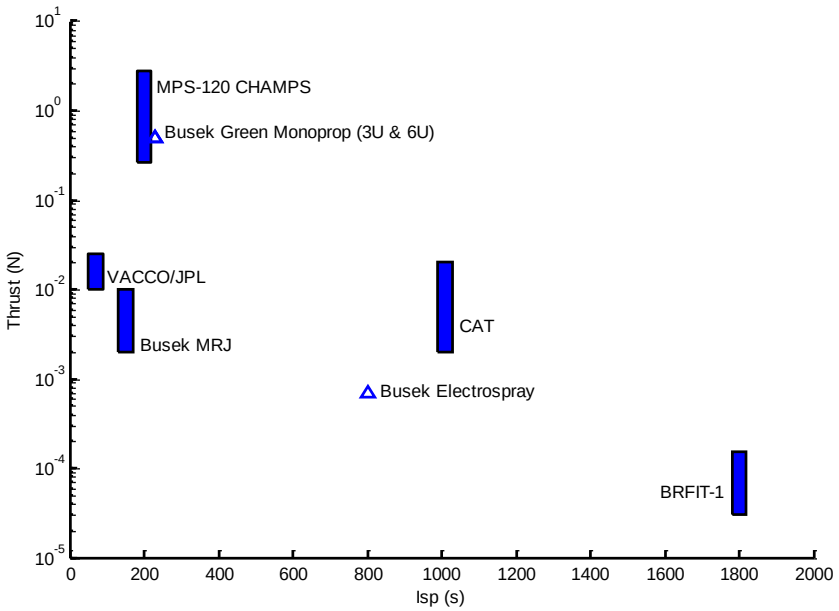

Figure 10. Thrust vs. Isp for all thrusters.

ΔV is a critical measurement used to determine how much thrust acceleration is necessary to perform an orbital maneuver. The ΔV for an electric propulsion thruster is given by the rocket equation,

$$V_{ex} = \frac{I_{sp} g_0}{1000}, \tag{9}$$

$$\Delta V = V_{ex} \log \frac{m_t}{m_d}, \tag{10}$$

ΔV is not dependent upon the power, only on thrust and $I_{sp.}$ However, the time to boost ΔV is dependent on the power level and is given by

$$t = \frac{m_f}{\dot{m}_{fp} P}, \tag{11}$$

Figure 11 shows ΔV versus fuel mass for the BRFIT-1 (assuming a constant I_{sp} of 1800 s) and the other seven thrusters. Figure 12 shows time to boost for the BRFIT-1 at different fuel masses and thrust levels. The results meet expectations; in order to perform high ΔV maneuvers, more fuel is required. It can be observed in Figure 12 that at higher thrust levels the time to change ΔV decreases, but at higher power levels the time to change ΔV increases.

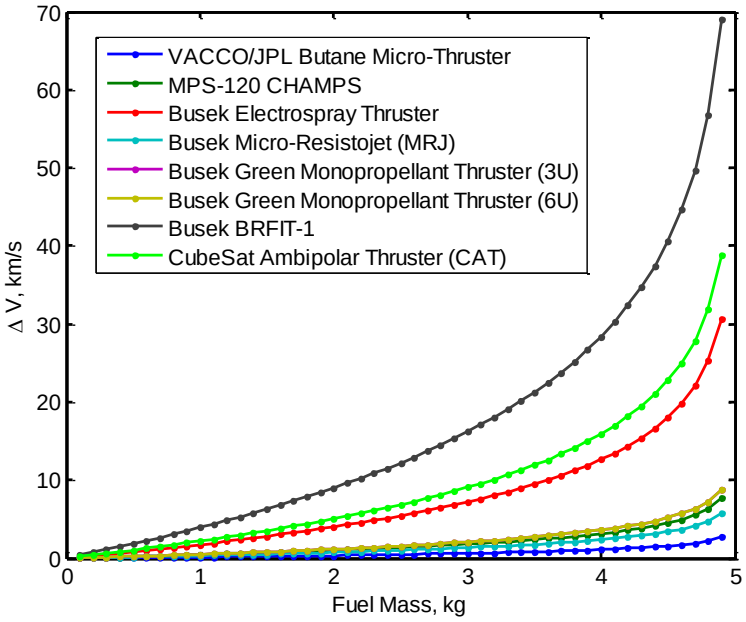

Figure 11. ΔV versus fuel mass for all thrusters.

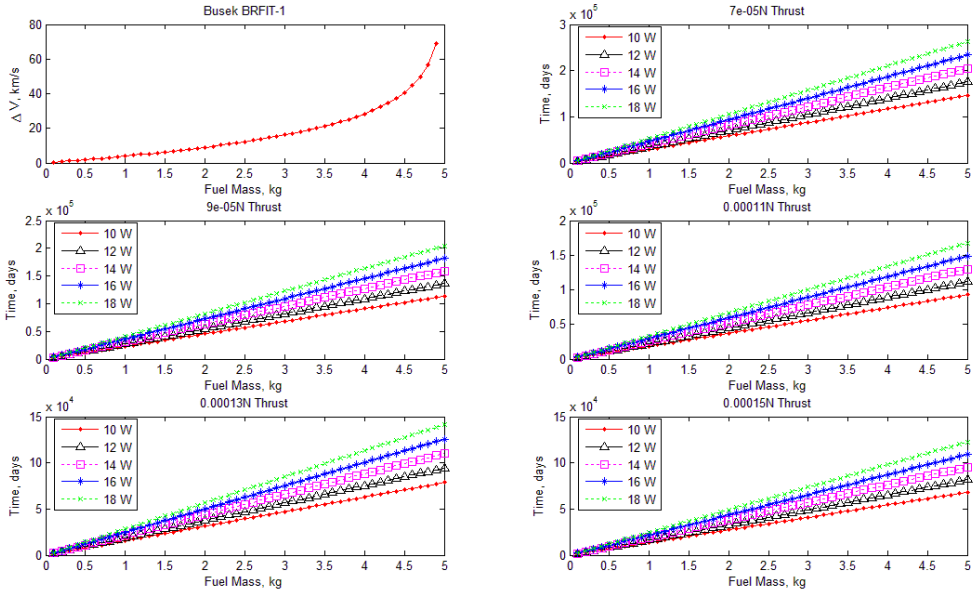

Figure 12. ΔV and time to boost ΔV for Busek BRFIT-1

Figure 18-23 in the Appendix give similar plots for the other seven thrusters. These plots show some similarities and differences compared to the BRFIT-1. For the CAT in Figure 18, the ΔV for fuel mass compared to the BRFIT-1 is much smaller. But comparing the time to boost, ΔV for the CAT thruster is an order of magnitude lower than the BRFIT-1. The thrust and power ranges are much higher than the BRFIT-1.

Figure 19 illustrates the performance of the CHAMPS thruster. ΔV to fuel mass is lower than the BRFIT-1 and CAT. The thrust range is much higher for CHAMPS and it has the lowest time to boost ΔV compared to all of the other six thrusters. Figure 20 shows both the 3U and 6U Busek Green Micropropellant thrusters. Like CHAMPS, both green Micropropellant thrusters have small ΔV per fuel mass. The thrust values are both 0.5 Newtons and the time to boost ΔV is in the range of a few days up to one week.

Figure 21 shows the Busek Micro-Resistojet. Compared to the other thrusters, the Micro-Resistojet's ΔV per fuel mass and time to boost ΔV are average and I_{sp} is small. Figure 22 shows the characteristics of the Busek Electrospray Thruster. This thruster has a comparable ΔV per fuel mass to the CAT thruster. The time to boost ΔV per fuel mass is smaller than CAT thruster by a magnitude of ten. Figure 23 depicts the performance of the VACCO/JPL butane thruster. This thruster has the smallest ΔV per mass of fuel out of all of the other thrusters. The time to boost ΔV for this thruster is similar to Busek's Green Micropropellant thrusters for similar thrust levels, but the VACCO/JPL thruster has much smaller power levels.

The escape time and mass of fuel needed to escape the Earth's sphere of influence were also evaluated for each thruster using standard equations. To determine the escape time, we calculated the ΔV required to reach Earth's sphere of influence from a 500 km orbit,

$$\Delta V = V_f - V_0, \tag{12}$$

where $V_0 = \sqrt{\frac{\mu}{(alt+Re)}}$ and $V_f = \sqrt{\frac{\mu}{r_f}}$.

After determining the required ΔV we compute the required mass of fuel and the time to escape

$$m_{req} = m_t - m_d, \tag{13}$$

$$t_{escape} = \frac{m_{req}}{\dot{m}_f}, \tag{14}$$

where $m_d = \frac{m_t}{10^{\frac{-\Delta V}{Vex}}}$.

Table 3 shows all of the thrusters with the time and required fuel mass to escape, as well as the volume of fuel required for each thruster.

Table 3. Thruster time, fuel mass, and fuel volume required to escape.

Thruster and Power Levels (W)	Time to Escape (days)	Mass of fuel required (kg)	Volume of fuel required (U)
VACCO/JPL Butane Micro-Thruster			
0.1	63.5833	5	8.9286
1.075	5.91473		
2.05	3.10163		
3.025	2.10193		
4	1.58958		
MPS-120 CubeSat High-Impulse Adaptable Modular Propulsion System (CHAMPS)System		4.9986	4.9006
1	0.16216		
1.75	0.092661		
2.5	0.064863		
3.25	0.049894		
4	0.040539		

Busek Electrospray Thruster		4.3512	4.3512
3	564.6211		
Busek Micro-Resistojet (MRJ)		4.9999	6.5788
3	8.5155		
Busek Green Monopropellant Thruster (3U)		4.9959	3.3986
20	8.5155		
Busek Green Monopropellant Thruster (6U)		4.9959	3.3986
20	0.26093		
Busek BRFIT-1		2.9825	0.96211
10	7314.6467		
12	6095.539		
14	5224.7477		
16	4571.6542		
18	4063.6926		
CubeSat Ambipolar Thruster (CAT)		4.008	
3	2298.1405		0.92564
77.25	89.248175		
151.5	45.507733		
225.75	30.540073		
300	22.981405		

To evaluate the mass and volume constraints of a realistic CubeSat mission, we assume a 3U CubeSat with a maximum payload of 5 kg. Typically the required volume for this size of CubeSat for the thruster, fuel, and extra battery is 1.4U. We assume the power will not exceed 20 W, so additional batteries to provide power for the thrusters can be omitted. Table 4 is a breakdown of the mass of the fuel and the fuel tank volume.

Table 4. Thruster and fuel mass and volume data. (Note: only includes thrusters that had mass and volume data available on the manufacturer's web site)

Thruster	Thruster Mass (kg)	Thruster Volume (cm^3)	Thruster Volume (U)	Fuel Density (g/cm^3)	Fuel Tank Volume (U)	Fuel Volume (cm^3)	Fuel Mass (kg)
MPS-120 CubeSat High-Impulse Adaptable Modular Propulsion System (CHAMPS)	1.6	1135	1.135	1.02	.38	380	.3876
Busek Electrospray Thruster	1.15	433.5	.433	1.00	.3	300	.300
Busek Micro-Resistojet (MRJ)	1.25	810	.810	0.76	.64	640	.4864
Busek Green Monopropellant Thruster (3U)	0.7	51.481	.0514	1.47	1.348	1348	1.981
Busek Green Monopropellant Thruster (6U)	2.7	51.481	.0514	1.47	1.348	1348	1.981

B. Trajectory Analysis

Figure 13-Figure 15 show trajectory simulation results for the thrusters in Table 2. Each thruster was simulated at constant thrust until escape from the Earth's sphere of influence, assuming an initial spacecraft mass of 5 kg. For the VACCO/JPL thruster, the MPS-120 CHAMPS, and the Busek MRJ, simulations were performed at each thruster's maximum thrust level. The CAT maximum power of 300 W is well beyond the capability of CubeSats in constant thrust operation, so this thruster was not simulated at maximum thrust. The CAT simulations employed a thrust of 2 mN, which corresponds to continuous 10 W operation[11].

The results of these simulations agree with the calculated ΔV results in Table 3. The Busek Green Monopropellant Thruster, the MPS-120 CHAMPS, the VACCO/JPL thruster, and the Busek Micro-Resistojet each required close to 5 kg of fuel (the total initial spacecraft mass) and less than 10 days to escape. The CAT and the Busek Electrospray thruster required less fuel and longer times: approximately 2.5 kg fuel and 144 days for the CAT, 2.9 kg fuel and 380 days for the Busek Electrospray thruster.

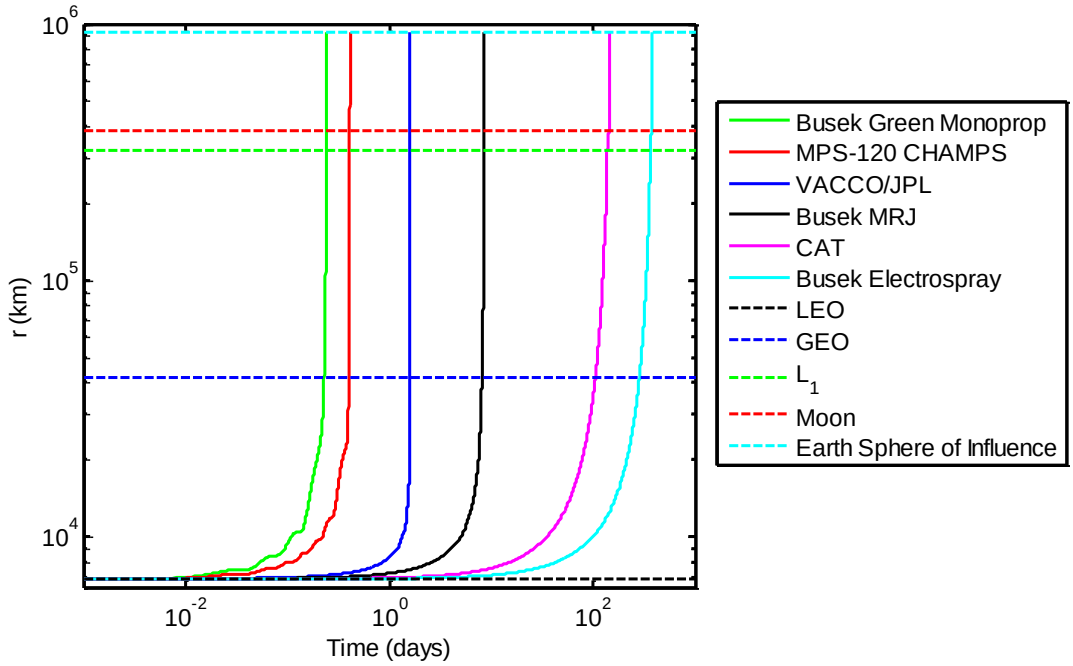

Figure 13. Radial distance versus time for the six trade thrusters at constant thrust.

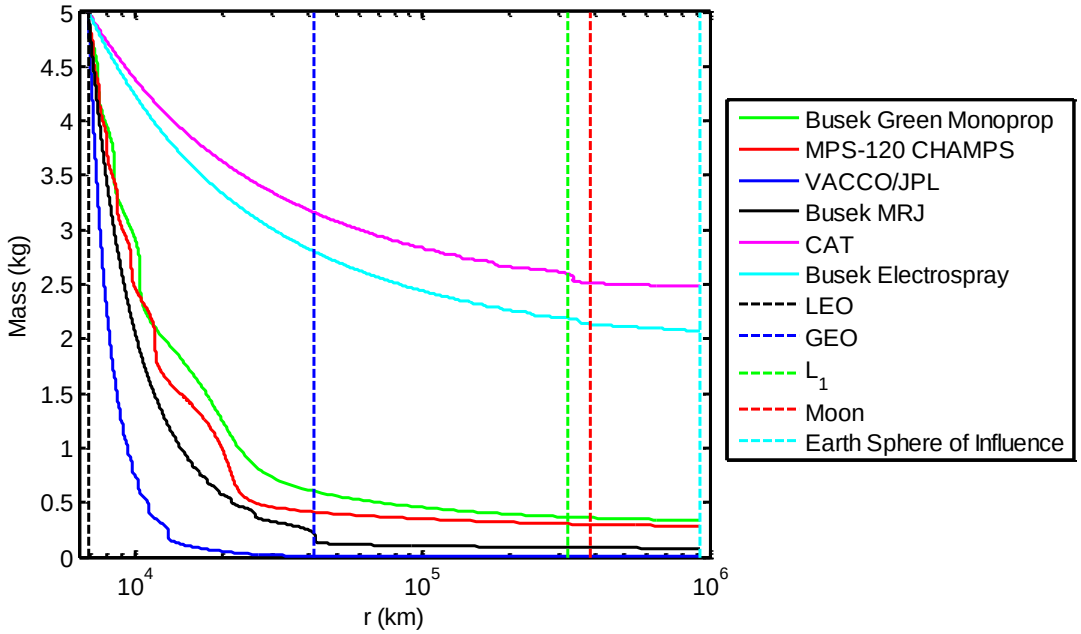

Figure 14. Mass versus radial distance for the six trade thrusters at constant thrust.

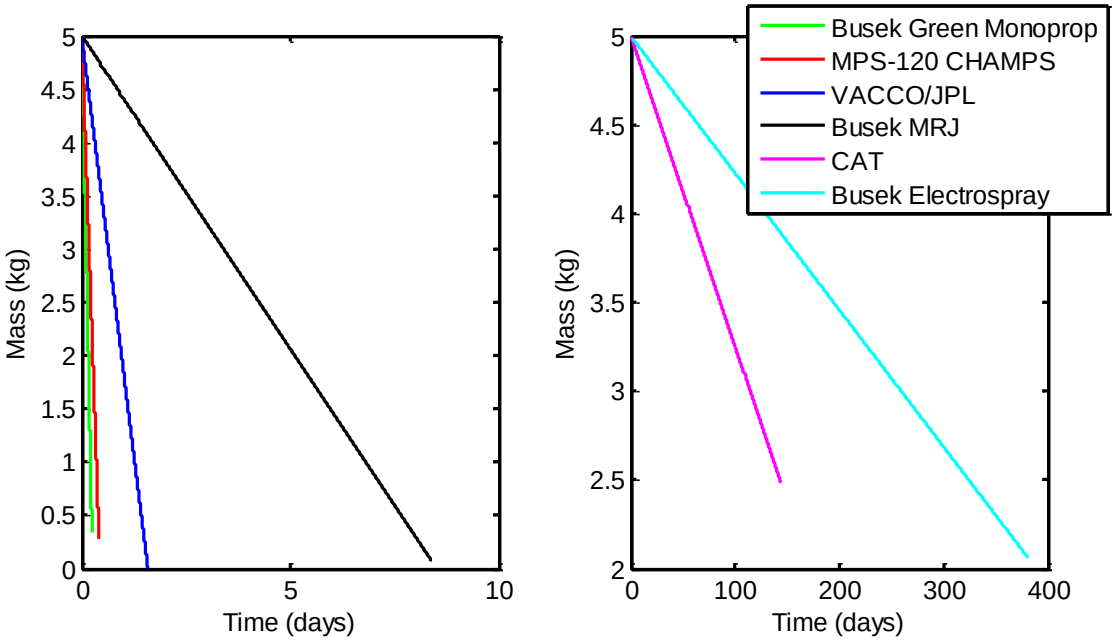

Figure 15. Mass versus time for the six trade thrusters at constant thrust.

Two more realistic fuel mass cases were also simulated. First, the case of a fixed spacecraft dry mass of 2.5 kg and initial fuel mass of 2.5 kg was considered. Under these conditions, only the Busek Electrospray thruster and the CAT were capable of reaching GEO, and only the CAT could approach the radius of the Earth's sphere of influence. The calculated time to 2.5 kg fuel burnout and the orbit radius at burnout are given in Table 8 in the Appendix.

Next, the case of fuel mass limited by spacecraft volume was also simulated. Table 4 gives an estimate of available fuel mass for each thruster, assuming typical mass and volume constraints of a 3U CubeSat. These

thruster-specific fuel mass limits were used for constant-thrust trajectory simulations. Figure 15 and Figure 16 show the simulation results for the four thrusters for which data was available. Under these system-level fuel mass and volume constraints, the Busek Green Monopropellant thruster is able to achieve the largest change in orbit radius: approximately 2,800 km in 2.5 hours.

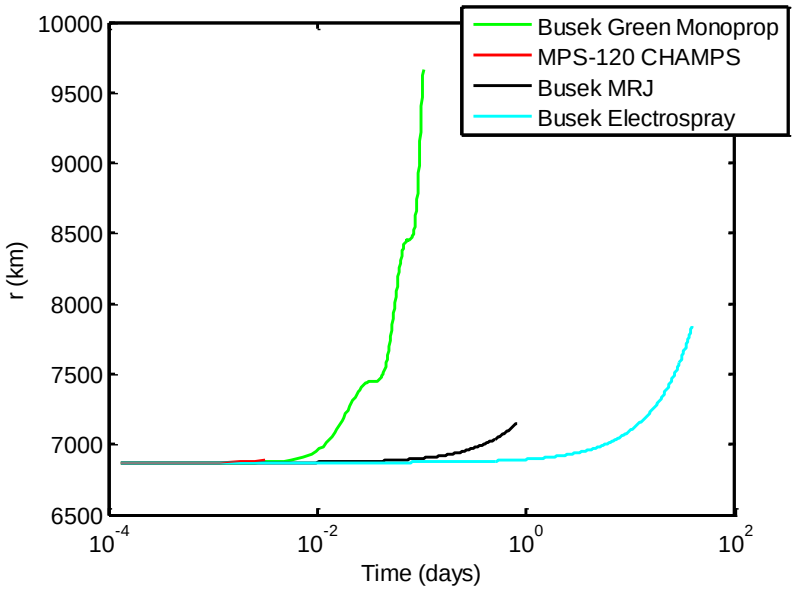

Figure 16. Radial distance versus time at constant thrust with realistic fuel mass limit for each thruster.

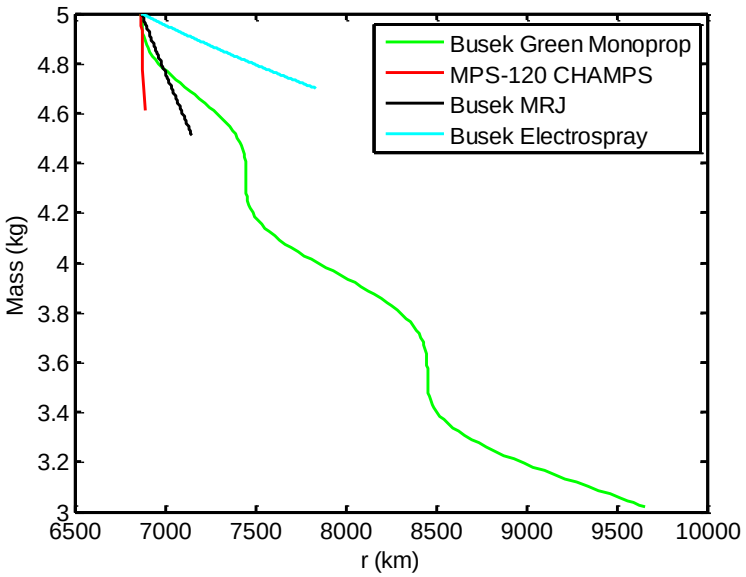

Figure 17. Mass versus time at constant thrust with realistic fuel mass limit for each thruster.

VIII. Conclusion.

This paper analyzed the orbit change capabilities of the Busek BRFIT-1 and seven other small propulsion systems. Several metrics and simulations were used to compare the thruster properties that contribute to orbit changes, including power, thrust, specific impulse, and fuel density.

Two-body trajectory simulations were used to compare four combinations of BRFIT-1 power and flow rate, which correlate to thrust and specific impulse, for a constant thrust trajectory from LEO. The strategy of applying thrust only near perigee was also considered, and trajectory simulations were performed for three flow rate cases at maximum power while applying thrust only within 40° of perigee. The constant thrust strategy at the highest power level achieved the fastest changes in orbit radius, but major orbit changes, such as LEO-to-GEO transfers or lunar missions were found infeasible due to thruster lifetime limitations. The perigee thrust cases required longer missions but shorter total thrusting times.

An optimized trajectory for the BRFIT-1 was obtained using a new method to minimize transfer time while maintaining realistic system-level constraints. A solution was found to achieve a LEO-GEO transfer in 7.3 years with only 0.4 kg of fuel. For other thrusters with a range of power and specific impulse levels, it may be possible to obtain comparable improvements over the constant thrust cases.

Next, the larger trade space for CubeSat propulsion systems was considered. Seven other small thrusters were considered, including a cold gas thruster, two monopropellant thrusters, a resistojet thruster, an electrospray thruster, and a permanent magnet helicon generated plasma thruster. The thrusters were compared graphically in terms of power, thrust, mass, and specific impulse. Using the rocket equation, each thruster's ΔV capability and time to boost were calculated for a range of power and fuel mass levels, and time to escape the Earth's sphere of influence was calculated. Also, a volume and mass analysis was conducted using CubeSat volume constraints. Trajectory simulations were performed for the seven trade thrusters, and the results agreed with the time and fuel to escape calculations.

These analyses illustrate the complexity of thruster selection and control strategy for CubeSat orbit changes. Table 5 gives an overview of our findings for the best operational modes for different mission goals. Table 6 lists the thruster properties that are most critical for different types of orbital maneuvers and matches the thrusters considered in this analysis with the types of CubeSat maneuvers for which they are best suited.

Table 5. Summary of CubeSat orbital maneuver goals and corresponding best thruster operational modes.

Orbital Maneuver Goal	Thruster Throttle Settings	Control Strategy
Minimize time (no system constraints)	High power, high fuel flow rate (high thrust, low Isp)	Continuous thrust at maximum available power (use Sun-synchronous orbit if possible)
Minimize time (power and fuel constraints)	Variable power and thrust	Optimized thrust arcs at most effective orbit locations
Minimize CubeSat complexity (no 3-axis attitude control system)	High power, high fuel flow rate (high thrust, low Isp)	Perigee thrust
Minimize total fuel	High power, low fuel flow rate (medium thrust, high Isp)	Perigee thrust

Table 6. Summary of best micro propulsion systems to achieve various types of CubeSat maneuvers.

Maneuver Type	Key Thruster Properties	Thrusters
Small maneuvers (e.g. station keeping, constellation deployment)	Low power, high fuel density	VACCO/JPL, MPS-120 CHAMPS, Busek Green Monopropellant, Busek Electrospray
Maximum orbit change given mass and volume constraints	High fuel density, small thruster volume	Busek Green Monopropellant
LEO to GEO	High Isp, range of power and thrust	BRFIT-1, Busek Electrospray, CAT
LEO to targets beyond GEO	High Isp, range of power and thrust	CAT

Appendix

Table 7. Trajectory simulation results for the BRFIT-1.

Power	Control Strategy	Flow Rate Thrust Isp	Time to GEO (35,700 km)	Fuel to GEO (35,700 km)	Time to L1 (322,000 km)	Fuel to L1 (322,000 km)	Time to r_Moon (384,000 km)	Fuel to r_Moon (384,000 km)	Time to r_SOI (925,000 km)	Fuel to r_SOI (925,000 km)
10 W	Constant Thrust	0.08 sccm 70 uN 900 s	2802 days	1.9191 kg	3803 days	2.6054 kg	3843 days	2.6328 kg	3980 days = 11 years	2.7264 kg
	Constant Thrust	0.02 sccm 40 uN 2000 s	5862 days	1.03 kg	8010 days	1.41 kg	8108 days	1.43 kg	8486 days = 23 years	1.4949 kg
18 W	Constant Thrust	0.08 sccm 150 uN 2000 s	1482 days = 4 years	0.979 kg	2137 days	1.4114 kg	2162 days	1.4280 kg	2256 days = 6.2 years	1.4904 kg
	Constant Thrust	0.02 sccm 85 uN 4400 s	2771 days	0.4715 kg	4109 days	0.6991 kg	4166 days	0.7088 kg	4378 days = 12 years	0.7749 kg
	Perigee Thrust ($\theta < 40°$)	0.08 sccm 150 uN 2000 s	10042 days = 27.5 years	0.5803 kg						
	Perigee Thrust ($\theta < 40°$)	0.04 sccm 85 uN 4400	11060 days = 30.3 years	0.3573 kg						
	Perigee Thrust ($\theta < 40°$)	0.02 sccm 85 uN 4400 s	18392 days = 50.4 years	0.2724 kg						

Table 8. Thruster trade trajectory simulation results. Columns 2 and 3 show time and final radius for a total fuel expenditure of 2.5 kg, starting from a 500 km near-circular orbit with constant thrust. Columns 4-10 show time and fuel expenditures to GEO, L_1, Moon mean radius, and the Earth's sphere of influence for applicable cases.

	Time to 2.5 kg Fuel Burnout	Final r (km)	Time to GEO (35,700 km)	Fuel to GEO (35,700 km)	Time to L1 (322,000 km)	Fuel to L1 (322,000 km)	Time to r_Moon (384,000 km)	Fuel to r_Moon (384,000 km)
VACCO/JPL Butane Micro-Thruster at 25 mN	0.7948 days	7806						
MPS-120 CubeSat High-Impulse Adaptable Modular Propulsion System (CHAMPS) at 2790 mN	.0203 days	10526						
Busek Electrospray Thruster	324 days	84128	272 days	2.0997 kg				
Busek Micro-Resistojet (MRJ) at 10 mN	4.26 days	9164						
Busek Green Monopropellant Thruster (3U and 6U)	0.1306	10401						
CubeSat Ambipolar Thruster (CAT) at 2 mN	143 days	511380	100 days	1.7526 kg	138 days	2.402 kg	143 days	2.486 kg

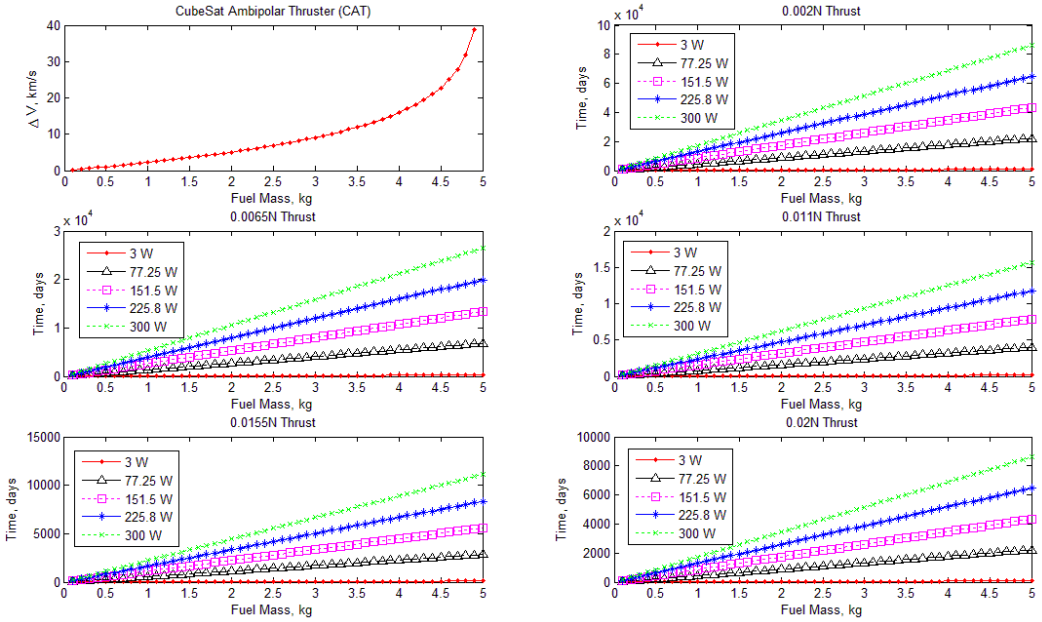

Figure 18. ΔV and time to boost ΔV for CAT

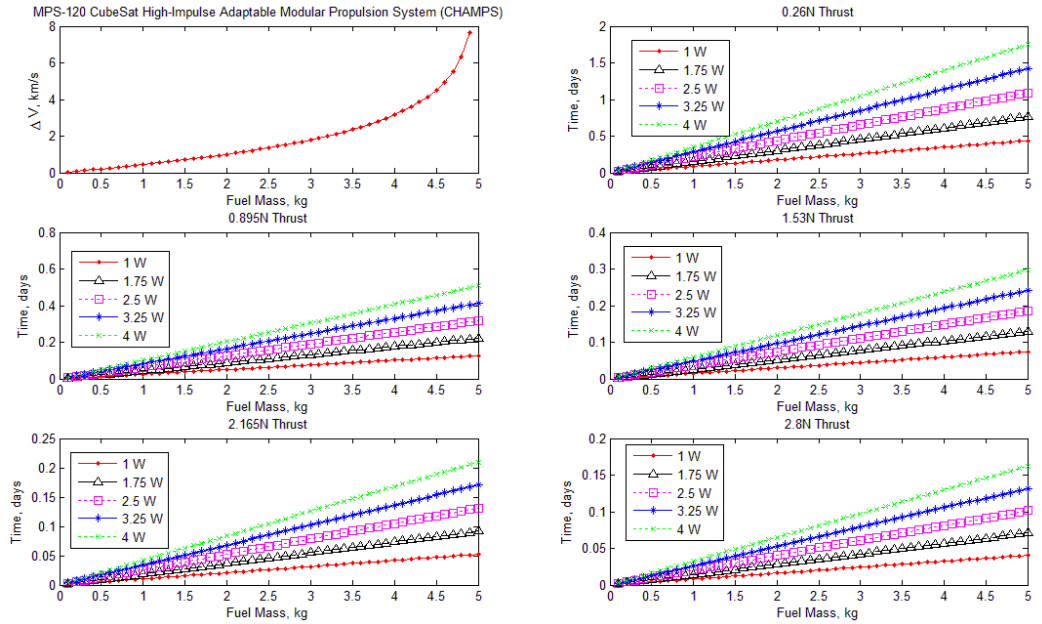

Figure 19. ΔV and time to boost ΔV for CHAMPS

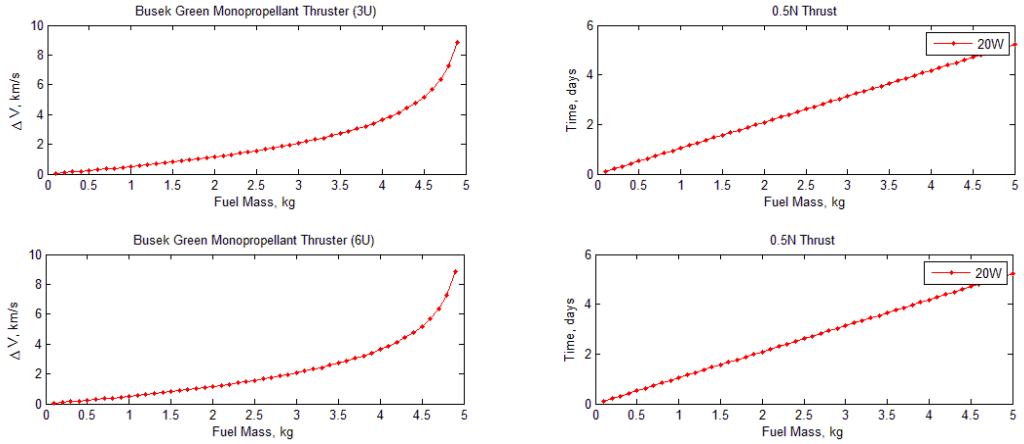

Figure 20. ΔV and time to boost ΔV for Busek Green Micropropellant Thrusters

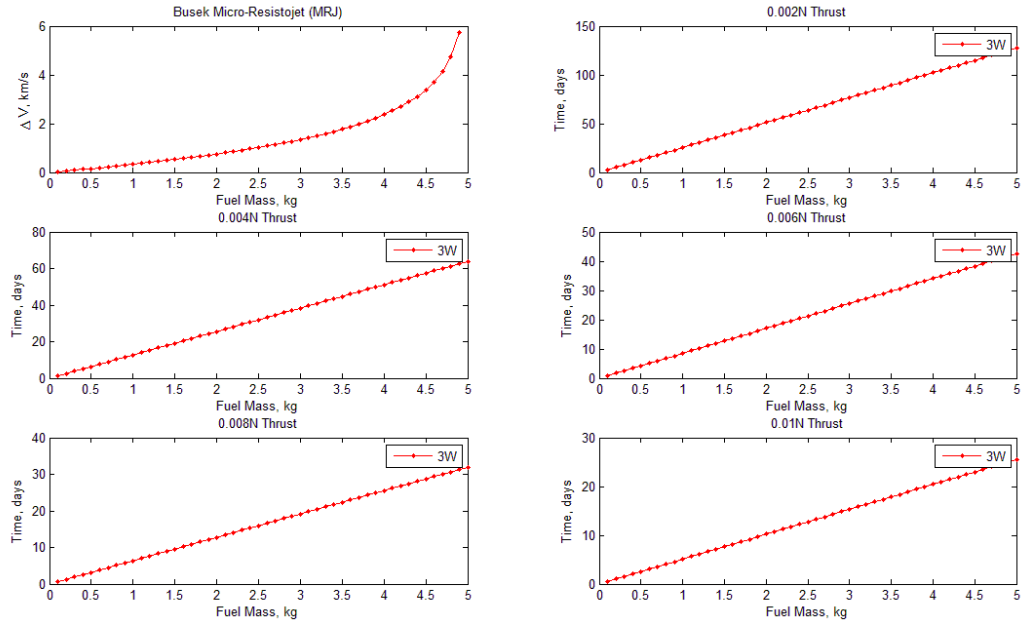

Figure 21 ΔV and time to boost ΔV for Busek Micro-Resistorjet

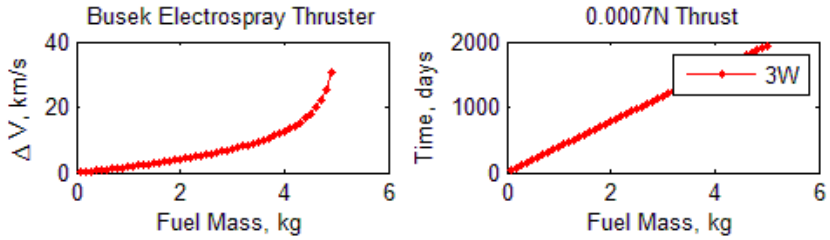

Figure 22. ΔV and time to boost ΔV for Busek Electrospray Thruster

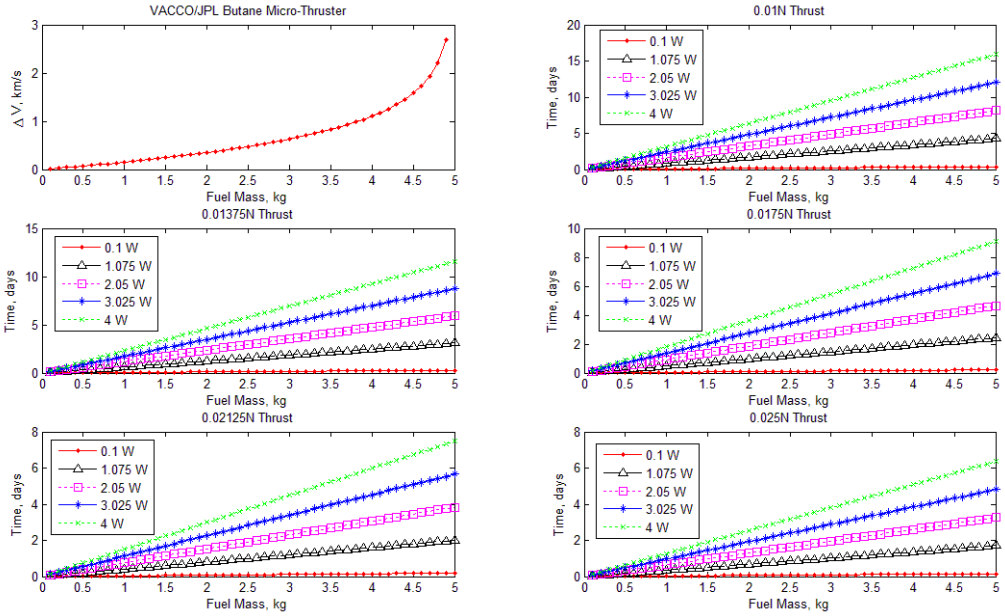

Figure 23. ΔV and time to boost ΔV for VACCO/JPL butane thruster

Acknowledgments

The authors acknowledge support by NASA cooperative agreement NNX13AR18A.

References

[1] Mueller, J., Hofer, R., and Ziemer, J., "Survey of propulsion technologies applicable to cubesats." *57th Joint Army-Navy-NASA-Air Force (JANNAF) Propulsion Meeting*, Colorado Springs, CO, 2010.

[2] Tsay, M., Hohman, K., Rosenblad, N., Ehrbar, E., and Robin, M.. "Micro radio-frequency ion propulsion system." *48th AIAA/ASME/SAE/ASEE Joint Propulsion Conference*, Atlanta, GA, 2012. AIAA 2012-3947.

[3] Spangelo, S. and Longmier, B., "BravoSat: Optimizing the Delta-V Capability of a CubeSat Mission with Novel Plasma Propulsion Technology", *Interplanetary Small Satellite Conference*, Pasadena, CA, 2013.

[4] Spangelo, S. and Longmier, B., "Optimizing Orbit Transfer Time using Thrust and Attitude Control for a CubeSat with Interplanetary Applications", *Interplanetary Small Satellite Conference*, Pasadena, CA, 2014.

[5] Mueller, J., Ziemer, J., Hofer, R., Wirz,, R. and O'Donnell, T., "A Survey of Micro-Thrust Propulsion Options for Microspacecraft and Formation Flying Missions", *5th Annual CubeSat Developers Workshop*, San Luis Obispo, CA, 2008.

[6] http://www.rocket.com/cubesat/mps-120 (accessed July 8, 2014)

[7] Schmuland, D.T., Carpenter, C., and Masse, R.K., "Mission Applications of the MRS-142 CubeSat High-Impulse Adaptable Monopropellant Propulsion System (CHAMPS)", *48th AIAA/ASME/SAE/ASEE Joint Propulsion Conference & Exhibit*, Atlanta, GA, 2012.

[8] Spence, D., Ehrbar, E., Rosenblad, N., Demmons, N., Roy, T., Hoffman, S., Williams, D., and Hruby, V., "Electrospray Propulsion Systems for Small Satellites", *27th Annual AIAA/USU Conference on Small Satellites*, Logan, UT, 2013.

[9] http://www.busek.com/technologies__therm.htm (accessed July 8, 2014)

[10] http://www.busek.com/index_htm_files/70008500_revD.pdf (accessed July 8, 2014)

[11] http://pepl.engin.umich.edu/thrusters/CAT.html (accessed July 8, 2014)

[12] Rathsman, P., Kugelberg, J., Bodin, P., Racca, G.D., Foing, B., and Stagnaro, L. "SMART-1: Development and lessons learnt." *Acta Astronautica*, Vol. 57, No. 2, 2005, pp. 455-468.

[13] Danby, J. M. A., *Fundamentals of Celestial Mechanics*, 2nd ed., Willmann-Bell, Richmond, VA, 2003, pp. 327–328.